Available online at www.sciencedirect.com
SCIENCE DIRECT®
Optics Communications 235 (2004) 421–434
OPTICS COMMUNICATIONS
www.elsevier.com/locate/optcom

Experimental and theoretical investigations on elliptically polarized dynamical transition states in the polarization switching of vertical-cavity surface-emitting lasers

Markus Sondermann [a,*], Thorsten Ackemann [a], Salvador Balle [b], Josep Mulet [b], Krassimir Panajotov [c,d]

[a] Institut für Angewandte Physik, Westfälische Wilhelms–Universität Münster, Corrensstr. 2/4, D-48149 Münster, Germany
[b] Instituto Mediterráneo de Estudios Avanzados (IMEDEA), Universitat de les Illes Balears, E-07071 Palma de Mallorca, Spain
[c] Department of Applied Physics and Photonics (TW ALNA), Vrije Universiteit Brussels, Pleinlaan 2, 1050 Brussels, Belgium
[d] Institute of Solid State Physics, 72 Tzarigradsko Chaussee Blvd., 1784 Sofia, Bulgaria

Received 1 December 2003; received in revised form 24 February 2004; accepted 25 February 2004

Abstract

The existence region of elliptically polarized dynamical states in the polarization dynamics of vertical-cavity surface-emitting lasers is investigated experimentally and theoretically. These states can occur in the vicinity of a polarization switching from the fundamental transverse mode with lower emission frequency to the mode with higher frequency. It is demonstrated experimentally that these states may occur in a single as well as in a double switching scenario. The existence of the dynamical states is shown to be independent from the ellipticity of the state of polarization at the lasing threshold. Furthermore, the influence of the detuning between the band gap and the cavity resonance on the occurrence of the dynamical states is investigated.

PACS: 42.25.Ja; 42.55.–f; 42.55.Px; 42.65.Sf

Keywords: Vertical-cavity surface-emitting lasers; Polarization; Non-linear dynamics

1. Introduction

The polarization dynamics of vertical-cavity surface-emitting lasers (VCSELs) has been a subject of high interest over the last years. Unlike in edge-emitting semiconductor lasers, the state of polarization (SOP) of the emitted light is not fixed

* Corresponding author. Tel.: +49-2518-333520; fax: +49-2518-333513.
E-mail address: sondema@uni-muenster.de (M. Sondermann).

0030-4018/$ - see front matter
doi:10.1016/j.optcom.2004.02.073

by geometrical constraints and a large variety of effects and dynamics concerning the SOP of the VCSEL radiation are observed (see e.g. [1] for a review). These effects occur in spite of the fact that the circular geometry is broken by unavoidable small linear anisotropies (see e.g. [2,3]) which favour the emission of a linear SOP. A phase anisotropy, often termed birefringence, induces a frequency splitting of modes of the same order but orthogonal linear polarization, whereas the amplitude anisotropy, or dichroism, results in different linear – *i.e., unsaturated* – net gains of these modes.

Probably the most striking phenomenon observed in experiments is the so-called polarization switching (PS) between two orthogonally linear polarized modes occurring at some point, when the injection current is increased gradually (e.g. [4–8]). The nature of the processes inducing PS has been mainly addressed within two lines of reasoning. One class of models explains PS in terms of the linear (unsaturated) gain and loss anisotropies which might be changed by thermal effects [5,6,9,10]. A different explanation takes into account explicitly the spin degrees of freedom of a semiconductor quantum well and considers two reservoirs of carrier populations with opposite spin from which photons of opposite helicity are emitted [11,12]. In the framework of this model, which is often called *spin-flip model* (*SFM*), PS is induced by spin dynamics and saturable dispersion under conditions of a weak coupling between the spin reservoirs. Linear SOP originate from the locking of left and right circular polarization to a fixed phase of either 0 or π. In this sense, PS is due to an instability of the phase with which the two fields decide to switch among these two solutions.

As a special feature of the latter model, the possibility of the occurrence of elliptically polarized dynamical states in the vicinity of a PS from the fundamental transverse mode with lower optical frequency (LF-mode) to the mode with higher optical frequency (HF-mode) is predicted for certain values of the anisotropies (rather low birefringence and dichroism) [12]. The scenario predicted in [12] is as follows: First, the steady state with a linear SOP gives way to an elliptical SOP if the current is increased. The elliptically polarized steady state then becomes unstable and dynamical and nonstationary states occur, in which the SOP is varying in time. The presence of these states can be detected in the optical spectrum as sidebands of the lasing line, which cannot be suppressed by means of a linear polariser alone. If the current is increased further, the laser switches to the HF-mode. In the existence region of the dynamical states there is no well defined SOP and the so-called fractional polarization drops to a value significantly smaller than one. Also other previous studies [13,14], based on the SFM, demonstrated that the elliptical steady states are linearly stable in a narrow current interval in the vicinity of a LF–HF PS and analyzed the Hopf bifurcation to a nonstationary SOP. In spite of these advances, the underlying mechanisms leading to the excitation of elliptical states followed by the sequence of dynamical SOP are not fully understood.

The experimental observation of a scenario that shows strong similarities to the predictions mentioned above has been reported recently [15]. However, the interpretation of the results obtained in [15] is complicated by the fact that the VCSEL studied there was already emitting in an elliptical but well defined SOP at the lasing threshold. It will be shown in this contribution that the dynamical states can occur independently of the ellipticity of the SOP at threshold. In addition, we provide direct proof in the time domain that the appearance of the sidebands is related to rather – but not completely – regular oscillations of the intensity of the polarization components. Furthermore, we will characterize different manifestations of dynamical states and their existence region in parameter space. The experimental results are compared with theoretical predictions. An extended version of the original spin-flip model [12] is used, which includes a frequency-dependent susceptibility [16] and hence allows for a simple description of the thermal shift of the cavity modes [17].

The paper is organized as follows: In the next section the experimental results will be reported. In Section 3 the theory and its predictions will be discussed. The last section gives a discussion and some concluding remarks.

2. Experiment

The VCSELs that were investigated in the experiments described here are gain guided commercial devices obtained from Emcore (model 8085-2010). The device aperture is 8 μm. This ensures fundamental transverse mode operation up to more than 200% above threshold. The emission wavelength is about 845 nm. The devices are mounted in a temperature controlled holder by which the temperature of the VCSEL package can be stabilised in a range from 6 to 70 °C. The light emitted by the VCSELs is collimated by an aspheric, anti-reflection coated lens and split into its orthogonal linear polarization components by means of a half-wave plate and a Wollaston prism. For projection onto circularly polarized components a quarter-wave plate is inserted after the collimation lens. For each of the linear polarization components the time averaged power is measured by low-bandwidth detectors. The optical spectrum is measured with a Fabry–Perot interferometer with a finesse of 150 and a free spectral range of 46 GHz. Back reflections into the VCSEL are prevented by an optical isolator with more than 60 dB suppression. For measuring the polarization resolved fast temporal dynamics a photodiode with a bandwidth of 20 GHz was used in one of the optical paths after the Wollaston prism. Due to the low sensitivity of the photodiode, the signal had to be amplified by 40 dB using two amplifiers (Agilent A83006A, 0.1–26.5 GHz) at the expense of losing the DC-information. The amplified signal was connected to a digital oscilloscope (LeCroy Wavemaster) with 6 GHz analogue bandwidth and a sampling rate of 2×10^{10} samples per second. Power spectra were recorded with a spectrum analyser of 20 GHz bandwidth (Anritsu MS2665C).

The SOP of a monochromatic wave can be expressed in terms of two characteristic angles [18]. One of these angles describes the tilting angle of the main axes of the polarization ellipse away from a basis vector corresponding to one of two orthogonally linear polarized basis states. The other angle gives the ellipticity of the SOP and is determined by the arc tangent of the main axes of the polarization ellipse. The modulus of the ellipticity angle ranges from 0 to $\pi/2$. This corresponds to linear and circular polarization, respectively. It was found theoretically in [18] that stationary steady states with a finite ellipticity angle are stable at the lasing threshold, if the main axes of birefringence and dichroism are misaligned. Such a misalignment can be induced and changed by mechanical stress [19]. Experimentally, the ellipticity angle of the SOP can be obtained by a measurement of the so-called normalised Stokes parameters (for a definition see e.g. [12]) from the relationship

$$S_{\mathrm{circ}} = \sin(2\chi),$$

where χ is the ellipticity angle and S_{circ} is the Stokes parameter giving the fraction of circularly polarized light.

In [15], the dynamical states were observed for a device that displayed an elliptically polarized stationary state at threshold with an ellipticity angle of 10°. It is an important question, whether the dynamical states can also be observed experimentally for other parameter values, i.e., for other values of linear dichroism and birefringence and especially for lower values of the ellipticity angle of the steady state at threshold. The latter might provide evidence for the existence of a scenario that is closer to the predictions of [12] than the results obtained in [15]. To induce the parameter changes, stress was applied to different devices with the method explained in [8,20]. With this method the linear anisotropies were changed until a PS from the mode with lower optical frequency to the mode with higher optical frequency occurred. It should be stated for clarity that it was not possible to achieve the latter result for all of the investigated devices, especially if the residual amplitude anisotropy (i.e., without applying additional mechanical stress) was large.

In Fig. 1 the polarization resolved power after projection onto the eigen directions of the polarization ellipse of the SOP at threshold is displayed for a device with an ellipticity angle of 5°. At threshold only the mode with lower optical frequency is lasing. As observed in [15], the power increases in *both* polarization components with increasing current due to the finite ellipticity. Simultaneously, the ellipticity angle increases with

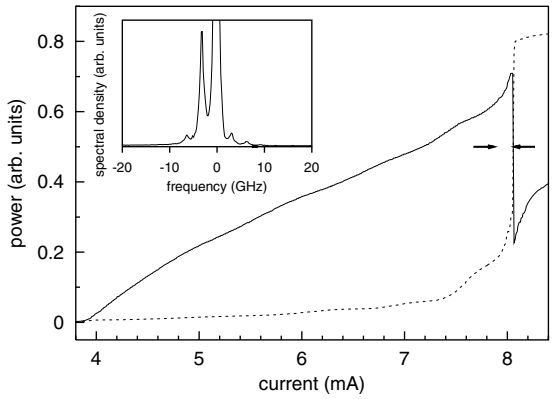

Fig. 1. Polarization resolved output power against current for projection onto the main axes of the state of polarization at threshold. The ellipticity angle at threshold is 5°. The solid (dashed) line corresponds to the power measured after projection onto the main axis of the SOP of the mode with lower (higher) optical frequency. The arrows indicate the current interval in which the dynamical states are observed. The inset shows the optical spectrum for a current of 8.02 mA after projection onto linear polarization minimizing the main peak. The largest peak is cut off for a better visualization of the smaller peaks. The amplitude of the highest peak is approximately 3.3 times larger than the amplitude of the largest side peak. The substrate temperature is set to 25 °C. The relative poor suppression ratio between the two polarization components after the PS is to some part due to the finite ellipticity (10° after the PS) and due to the fact that the principal axis of the polarization ellipse changed by 20° between threshold and the PS.

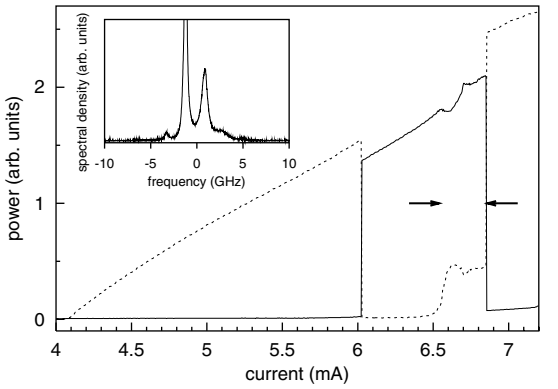

Fig. 2. Same as Fig. 1 but for a different device with an ellipticity angle $\leqslant 1°$ at threshold. The inset shows the optical spectrum for a current of 6.66 mA after projection onto linear polarization. The largest peak is cut off for a better visualization of the smaller peaks.

increasing current (such a behaviour has been predicted for steady states with nonzero ellipticity in [18]). First, this increase takes place rather slowly and with an approximately constant slope. At a current value of 7.4 mA ($\chi = 15°$) the slope of the ellipticity angle versus current drastically increases. In LI-curves measured by projection onto linear polarization states, this increase of ellipticity manifests itself by an increase of the slope of the power in the weaker linear polarization component, i.e., by a strong – though still continuous – increase in power (see Fig. 1). The ellipticity angle reaches its maximum value of 24° at 7.95 mA. At an injection current of 7.89 mA sidebands emerge in the optical spectrum (see left arrow in Fig. 1). They indicate the onset of dynamical states. The emergence of the sidebands coincides with a decrease of the fractional polarization. So far the observations match the results of [15,21]. In contrast to the latter works, in this laser the sidebands disappear directly at the point of the PS (8.05 mA, right arrow in Fig. 1). After the PS, the fractional polarization increases again. The ellipticity angle drops down to 10° directly after the PS.

By application of the strain method introduced in [8] to another device the scenario depicted in Fig. 2 has been encountered. At threshold, the lasing mode is the HF-mode. It can be completely suppressed by means of a linear polariser within the limits of our experimental setup. The ellipticity angle is smaller than 1° (the 'background' contribution due to imperfections in the setup is about 0.6°), i.e., the SOP can be regarded as linearly polarized. In [19] it was reported that all of the investigated VCSELs had a SOP with a small but finite residual ellipticity angle. In [6] the investigated VCSELs had an ellipticity angle of '1° or less' except for the ones with a very small birefringence (in that case it was 5–10°). At increasing current, at first a PS to the LF-mode occurs. Up to a current of 6.5 mA – i.e., in a current range extending beyond the first PS – the ellipticity stays below 4°. Also dynamical states do not appear at the first PS. If the current is increased further (beyond 6.5 mA), the ellipticity angle strongly increases (see also the increase of power in the weak linear polarization component about 6.4 mA) and

reaches about 22° before the second PS. At a current value of 6.55 mA sidebands appear in the optical spectrum and the fractional polarization decreases strongly (the minimum value is about 0.6). The sidebands disappear at the second PS, which is a switching back to the HF-mode. The fractional polarization increases again after the PS and the ellipticity drastically decreases. Hence, it can be concluded that the scenario reported here is qualitatively similar to the one observed for a single PS from the LF- to the HF-mode.

The results obtained so far indicate that the existence of elliptically polarized and of dynamical states before a LF–HF PS does not depend qualitatively on the initial ellipticity of the SOP at threshold, i.e., the observations confirm the core of the predictions of [12] for the transition scenario. However, the question whether the dynamical states or sidebands, respectively, disappear at the PS or at slightly higher currents as well as the magnitude of the sidebands in the optical spectrum (not discussed in detail here, but compare the inset in Fig. 1 with Fig. 4 of [15]) might be linked to the ellipticity angle of the SOP at threshold. This point would deserve further, more detailed investigations. However, the mechanical design of our VCSEL mount is not elaborate enough to allow for a continuous, stable and reproducible variation of the strain parameter over larger parameter regions.

In some of the experiments a fast digital oscilloscope was available, allowing for an investigation of the temporal dynamics during the emission of the dynamical states. In Fig. 3 the dynamics is illustrated for the same device that is presented in Fig. 2 but for a different run of the experiment. The properties of the SOP at threshold and the switching scenario are almost the same as in Fig. 2 but the PS occurs at slightly higher switching currents. This is presumably due to slightly different linear anisotropies. As depicted in Fig. 3(a), a strong peak at a frequency of about 2.1 GHz is observed in the power spectrum for projection onto the linear polarization directions corresponding to maximum and minimum time averaged power, i.e., onto the main axes of the polarization ellipse of the time averaged SOP. This frequency corresponds to the distance of the sidebands in the optical spectrum (in optical frequencies) and can therefore be interpreted as the beating frequency between the different 'modes' which are oscillating at adjacent frequencies. We interpret this frequency difference as the 'effective birefringence', i.e., the sum of the linear birefringence observed at threshold and the non-linear contributions due to saturable dispersion and spin dynamics [6,15,22–24]. Since several sidebands are excited in the optical spectrum (see also inset of Fig. 2), also higher harmonics of the beating frequency are observed in the power spectrum.

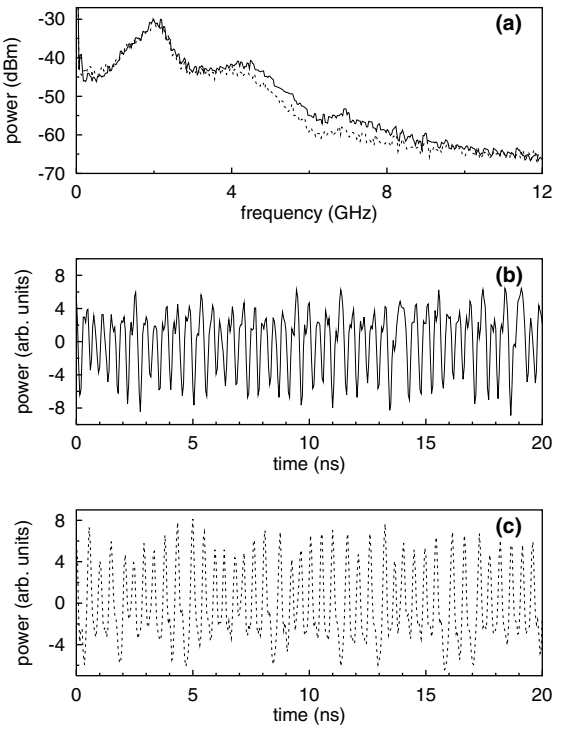

Fig. 3. Power spectra (a) and time series (b,c) of the dynamics in the regime of the emission of dynamical states. The solid (dashed) line in (a) represents the power spectrum after projection onto the linearly polarized state with maximum (minimum) dc-output. The corresponding time trace is given in (b) and (c), respectively. All data were measured after 40 dB amplification. Note that the two time traces have not been obtained simultaneously and that the DC-information is lost due to the amplification.

Corresponding to these frequencies, pronounced oscillations are observed in the time domain (see Fig. 3(b) and (c)). The time traces have not been obtained in a simultaneous measurement.

Hence they contain no information about the correlation properties of the dynamics. The oscillation at 2.1 GHz is observed for projection onto both of the polarization main axes.

From these observations the following conclusions can be drawn: First, due to the rather regular temporal oscillation at the frequency splitting of the sidebands in the optical spectrum, the sidebands can be considered as a (nearly) locked state and not as independent modes. Second, the presence of these oscillations in both linear polarization components hints to an oscillation of the characteristic polarization angles, i.e., ellipticity and orientation of the SOP. This issue is discussed further in Section 3.

The occurrence regime of the dynamical states is not necessarily restricted to the vicinity of a PS. This is demonstrated in Fig. 4. As depicted in part (a), the LF-mode is lasing at threshold. If the current is increased, this mode remains lasing until a current value of $\approx$8 mA. At this current level, a strong increase of power in the orthogonal polarization direction is observed. At the same time, for current values larger than 8 mA sidebands in the optical spectrum are observed (see inset in Fig. 4(b)). Fig. 4(b) shows the fractional polarization that corresponds to part (a) in dependency of the current. The fractional polarization is defined as the sum of the squares of the time average of the three normalized Stokes parameters [12]. At current levels close to the lasing threshold, the fractional polarization is reduced due to the strong impact of the non-lasing mode that is driven by spontaneous emission. For slightly higher current values, the fractional polarization reaches about 0.97 and remains at first on that level. The latter value corresponds to an almost pure SOP. At about 8 mA, i.e., when the sidebands in the optical spectrum emerge, the fractional polarization drops to lower values and remains approximately constant at 0.53 for increasing current. A recovery of the fractional polarization to a value close to unity, as it occurs for PS, is not observed. Here, a different kind of polarization instability is observed, i.e., a large current interval in which apparently none of the purely polarized steady states is stable. A scenario like the one described here has been predicted in [12].

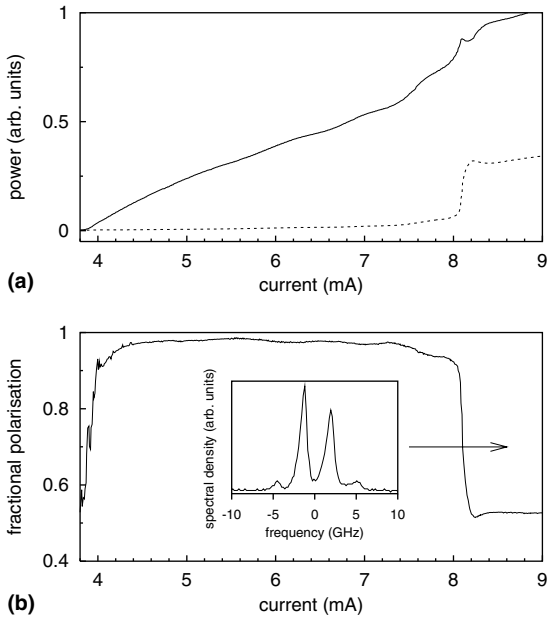

Fig. 4. (a) Same as Fig. 1 for the same device, but for slightly different stress conditions, i.e., slightly larger birefringence (ellipticity angle at threshold of 2°). The corresponding current dependence of the fractional polarization is displayed in (b). The inset shows the optical spectrum at 9 mA for projection onto a linear polarization state minimizing the main peak. High order modes are excited for $I > 9$ mA, however, their frequency is not in the spectral window displayed. First, the ellipticity angle slightly decreases with increasing current and then increases to 5° at about 8 mA.

We want to finish this section with a discussion of the influence of the substrate temperature, which influences the detuning between the band gap of the gain material and the cavity resonance of the laser (e.g. [5]), on the occurrence of the dynamical states. For this, we need to measure the characteristics of the VCSEL in a two-dimensional parameter space (current and temperature) over an extended range. It has been tried to implement this measurement for a device in which the ellipticity at threshold is adjusted to be small by applying stress. However, these attempts were not successful. This is presumingly due to some mechanical relaxation or change inside the VCSEL package and/or the special mounting that has to be used for the method introduced in [8]. The problem of mechanical stability is particularly severe in this

case, since the temperature of the mount is changed over a quite sizable range (60°). The stress relaxation led to a change of the linear anisotropies and thus to a change of the dynamics of the devices before the measurements were completed.

Hence, these temperature dependent investigations were performed using a rather rigid VCSEL holder, which was designed such that the additional stress by the mounting is minimized and constant and reproducible. The experiment was performed on the VCSEL that was also investigated in [15]. The results are reported in Fig. 5. For increasing temperature a clear decrease of the width of the current interval in which the dynamical states are excited is observed. At low substrate temperatures (10–15 °C) the width of the current interval where dynamical states occur is about 0.7 mA. At a substrate temperature of about 60 °C the dynamical states are observed in a rather small interval (0.1 mA) in the vicinity of the PS. In order to prevent a possible damage of the device under investigation, the substrate temperature was not raised to higher values. However, it can be conjectured from extrapolating the data that the interval with dynamical states will vanish if the temperature is increased further.

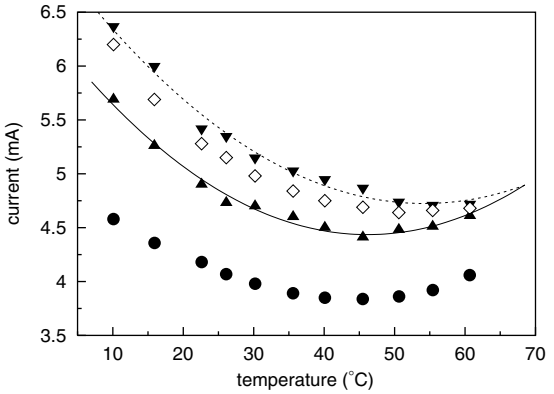

Fig. 5. Regime of occurrence of dynamical states in dependence of the substrate temperature for a device with an ellipticity angle of 10° at threshold. The lasing threshold is indicated by filled circles. The point of the polarization switching (defined as the current value where both modes emit with equal time averaged power) is marked by open diamonds. Upward (downward) triangles indicate the beginning (end) of the current interval with dynamical states. The solid and dashed lines represent the results of a second order polynomial fit to the two latter data sets. The investigated device is the same as in [15].

Although the ellipticity angle of the SOP at threshold is quite large (10°), it is the advantage of the device investigated in [15] and in Fig. 5 that it exhibits the dynamical states without applying additional stress. By applying stress, a linearly polarized SOP at threshold could also be achieved for this device. However, the linear anisotropies where then so large that a PS was not observed any more.

3. Theory

In this section we want to compare the experimental results with the predictions of an extended version of the spin-flip model that includes a realistic semiconductor susceptibility [17]. Thanks to the frequency dependence of the susceptibility one is capable to correctly describe changes in the relative position between the cavity resonance and the gain curve. Hence, the thermal shift of resonances due to temperature changes as they often occur in experiments are described in a simple way. The choice of the spin-flip model is also motivated by the fact that it is to our knowledge the only model worked out in the literature which is capable of treating explicitly the phase relation between circularly polarized states. Especially, dynamical states have (to our knowledge) not been reported in the framework of other models until now. The latter feature is obviously important if one has to account for the experimentally observed feature that the degree of ellipticity might vary. Furthermore, the model used here could also successfully reproduce the polarization properties observed in the case of lasing of both polarization modes at threshold [25] and for PS from the HF-mode to the LF-mode [26]. In the two latter works, the experiments were performed on devices of the same type and manufacturer as the ones used here.

Under fundamental transverse mode operation, the evolution of the circularly polarized components of the electric field $E_{\pm}$ (slowly-varying envelopes) and the electronic densities $D_{\pm}$ with opposite spin (normalised to the transparency density N_t) are governed by [17,27,28]:

$$\dot{E}_{\pm}(t) = -\kappa E_{\pm} + \mathrm{i}\frac{a\Gamma}{2}\chi_{\pm}\left(\Omega + \mathrm{i}\frac{\dot{E}_{\pm}}{E_{\pm}}, D_{+}, D_{-}\right)E_{\pm} - (\gamma_a + \mathrm{i}\gamma_p)E_{\mp} + \sqrt{\beta_{\mathrm{sp}}D_{\pm}}\xi_{\pm}(t), \quad (1)$$

$$\dot{D}_{\pm}(t) = \frac{1}{2}\mu\frac{I_{\mathrm{t}}}{eN_{\mathrm{t}}} - AD_{\pm} - BD_{\pm}^2 \mp \gamma_j(D_{+} - D_{-}) + a\,\mathrm{Im}\,\chi_{\pm}\left(\Omega + \mathrm{i}\frac{\dot{E}_{\pm}}{E_{\pm}}, D_{+}, D_{-}\right)|E_{\pm}|^2. \quad (2)$$

The electronic densities with opposite spin interact with circularly polarized light with different helicity through the frequency dependent susceptibility $\chi_{\pm}$ [16,17]. We use analytical expressions for $\chi_{\pm}$ obtained in [16] that describe the gain and refractive index spectra as

$$\chi_{\pm}(\omega_{\pm} + \Omega, D_{\pm}) = -\chi_0\left[\ln\left(1 - \frac{2D_{\pm}}{u_{\pm} + \mathrm{i}}\right) + \ln\left(1 - \frac{D_{+} + D_{-}}{u_{\pm} + \mathrm{i}}\right) - \ln\left(1 - \frac{b}{u_{\pm} + \mathrm{i}}\right)\right], \quad (3)$$

where

$$u_{\pm} = \frac{\omega_{\pm}}{\gamma_{\perp}} + \Delta + \sigma(D_{+} + D_{-})^{1/3}, \qquad \Delta = \frac{\Omega - \omega_{\mathrm{t}}}{\gamma_{\perp}}. \quad (4)$$

Δ is the detuning between the cavity resonance Ω and the nominal transition frequency ω_{t} of the band gap, normalized to the material polarization decay rate $\gamma_{\perp}$. Thus, the difference in thermal shift of the frequency of the gain maximum and of the cavity resonance can be modelled by a variation of Δ. Δ increases with temperature since the redshift of the cavity resonance increases faster with temperature than the redshift of the band gap frequency [5]. σ (fixed to 0.2) describes band-gap shrinkage and b (fixed to 10^4) is a background contribution to χ without pumping. Spin-flip processes that reverse the electron spin directly couple the two carrier reservoirs. This effect is phenomenologically accounted for by means of the spin-flip rate γ_j. μ is the injection current normalized to the transparency current (I_{t}), e is the electron charge. The linear contributions to the birefringence and dichroism are γ_p and γ_a, respectively. In the framework of this model γ_a is a pure loss anisotropy. The differences in material gain due to the frequency splitting between the modes are incorporated by the optical susceptibility $\chi_{\pm}$. The rest of parameters are the cavity losses κ, the effective gain constant a, the confinement factor Γ (fixed to 0.045), the non-radiative and bimolecular recombination rates of the carriers A and B and the spontaneous emission rate β_{sp}. Finally, $\xi_{\pm}(t)$ are white Gaussian random numbers with zero mean and delta correlated in time that model spontaneous emission processes.

For convenience, the simulations have been performed in the circular polarized basis. To obtain expressions for the linearly polarized components one has to use the relations $E_{\parallel} = (E_{+} + E_{-})/\sqrt{2}$, $E_{\perp} = (E_{+} - E_{-})/(\mathrm{i}\sqrt{2})$, where steady state solutions of $E_{\pm}$ are of the form $E_{\pm}(t) = Q_{\pm}e^{-\mathrm{i}(\omega_{\pm}t \pm \psi)}$ with $Q_{\pm}$ being the amplitude of the field and ψ the phase with which the circularly polarized fields lock. If $\gamma_p > 0$, $E_{\perp}$ corresponds to the LF-mode and $E_{\parallel}$ corresponds to the HF-mode. The parameters used for the simulations are given in the figure captions and can be considered to be typical VCSEL parameters. The spin flip rate γ_j is taken as a fit parameter. It is found that the experimentally observed dynamics can be reproduced, if a rather low value of some tens of 10^9 s^{-1} is assumed. We stress that this choice does not only allow for a reproduction of the experimental results presented here but also for a reproduction of correlation properties during two-mode emission [25] and of a drop in total output power at a PS from the HF- to the LF-mode [26].

First, we want to discuss the typical properties of the dynamics during the emission of the dynamical states (see Fig. 6). The linear anisotropies have been chosen to be of the same order as for the experimental results of Fig. 3. Panel (a) displays the optical spectra after projection onto linearly polarized states, which exhibits several sidemodes that are typical for this dynamical regime (see also [12]). The time traces of the corresponding intensities are given in panel (b) and the power spectra in panel (c) of Fig. 6, respectively. As in the ex-

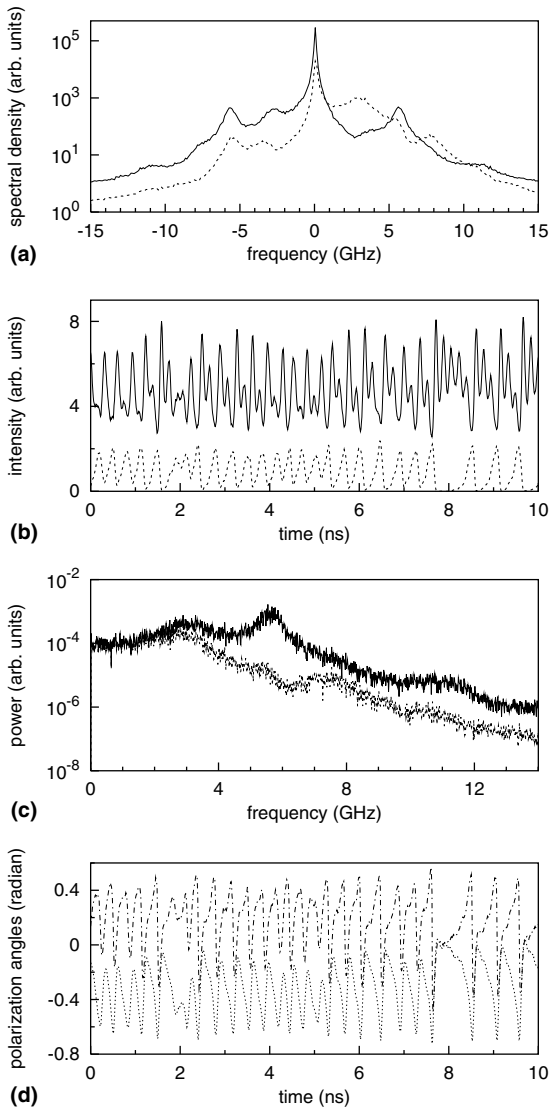

Fig. 6. Spectra and temporal evolution for projection onto linearly polarized states during the emission of the dynamical states. The optical spectra are shown in (a), where the direction corresponding to the linearly polarized mode with lower (higher) optical frequency is denoted by a solid (dashed) line. The temporal evolution of the corresponding field intensities is displayed in (b), whereas in panel (c) the power spectrum calculated from the time traces (total integration time 2 μs) is shown. The temporal evolution of the polarization angles is given in (d), where a dotted (dash-dotted) line represents the ellipticity (orientation) angle of the state of polarization. The parameters are $\gamma_a = 1$ ns^{-1}, $\gamma_p = 9$ ns^{-1}, $\gamma_j = 20$ ns^{-1}, $\Delta = 0$, $A = 0.5$ ns^{-1}, $B = 1$ ns^{-1}, $\kappa = 300$ ns^{-1}, $a = 2.5 \times 10^4$ ns^{-1}, $\gamma_\perp = 10^4$ ns^{-1}, $\beta_{sp} = 10^{-6}$ ns^{-1}. The current is 1.9 times the threshold value.

periments, the power spectra exhibit pronounced components at the beating frequency of adjacent side modes and its multiples. The corresponding oscillations are observed in the time traces. The computation of a cross correlation function reveals that the intensities in the orthogonal linear polarization directions have a correlation of −0.76 at zero time delay, i.e., they are strongly anticorrelated. As in the experiment, the oscillations are rather – but not totally – regular.

Unlike in the experiment, in the simulations the time resolved ellipticity and orientation angle can be easily computed from the time series of the complex optical field components [12]. The result of this procedure is displayed in Fig. 6(d). Both polarization angles are strongly oscillating. Their oscillation is also strongly anticorrelated. The fractional polarization, which is defined as the sum of the squares of the time averaged Stokes parameters [12], has a value of 0.45.

As a next step, we want to investigate the effect of a variation of the detuning Δ on the occurrence of the dynamical states. We start with a description of the stability properties obtained from a linear stability analysis of the linearly polarized solutions. The results are depicted in Fig. 7, where the linear anisotropies have been chosen to match the experimental ones of Fig. 5. Within the investigated detuning range, only the LF-mode is stable at threshold. The scenario that is observed for increasing current depends on detuning. For $\Delta < 0$ the LF-mode becomes unstable and the system enters a region where both linearly polarized modes are unstable. If the current is increased further, the HF-mode becomes stable. The current at which this mode becomes stable increases strongly with decreasing detuning. For $\Delta > 0$ the system enters first a region of bistability and then a region where only the HF-mode is stable.

For selected detuning values simulations including noise have been performed, where the current has been scanned from threshold to four times threshold for fixed detuning. The current value at which a PS to the HF-mode is observed is indicated in Fig. 7 by a triangle. For detuning values between $\Delta = 0$ and $\Delta = 1$ the switching current is higher than the current at which the LF-mode loses its linear stability. At the latter current

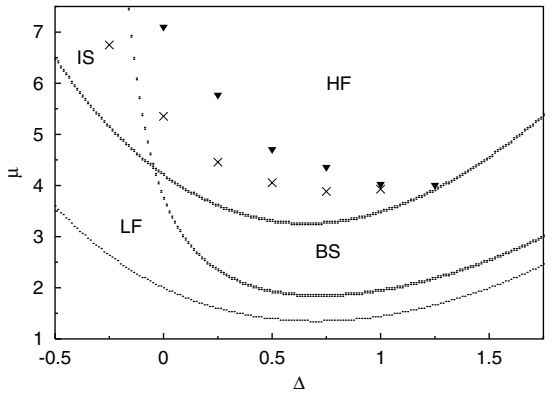

Fig. 7. Stability diagram of polarization state as a function of detuning Δ and current normalised to its transparency value. The stability properties of the linearly polarized solutions were determined by a linear stability analysis. In the area labelled HF (LF) only the linearly polarized mode with higher (lower) optical frequency is stable. In the area labelled BS (IS) both modes are stable (unstable). The triangles indicate the point where PS occurs in simulations including spontaneous emission noise. Crosses indicate the appearance of dynamical states. The parameters are $\gamma_a = 1$ ns^{-1}, $\gamma_p = 15$ ns^{-1}, $\gamma_j = 30$ ns^{-1}, $A = 0.1$ ns^{-1}, $B = 1$ ns^{-1}, $\kappa = 300$ ns^{-1}, $a = 6 \times 10^4$ ns^{-1}, $\gamma_\perp = 2 \times 10^4$ ns^{-1}, $\beta_{sp} = 10^{-6}$ ns^{-1}.

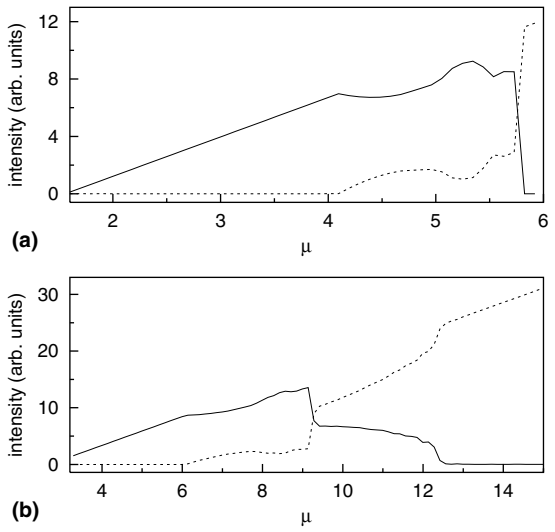

Fig. 8. Time averaged LI-curve after projection onto linear polarization states. The polarization direction corresponding to the mode with lower (higher) optical frequency is denoted by a solid (dashed) line. The parameters are the same as in Fig. 7 and $\Delta = 0.25$ in (a), $\Delta = -0.25$ in (b). Dynamical states appear at $\mu \approx 4.5$ in (a) and at $\mu \approx 6.75$ in (b).

value, an elliptically polarized steady state starts lasing. If the current is increased, the elliptically polarized steady state gives way to a dynamical state (indicated by a cross in Fig. 7), which is observed until the PS. A typical LI-curve is displayed in Fig. 8(a). At threshold, the linearly polarized LF-mode is selected. The appearance of a signal in both polarization components at about $\mu = 4$ indicates the transition to an elliptically polarized state. Then, at $\mu \approx 4.5$ sidebands appear in the optical spectrum. Finally, a PS to the HF-mode takes place. This scenario matches qualitatively the experimental findings.

For $\Delta \geqslant 1.25$ the PS is directly from the LF-mode to the HF-mode, i.e., neither elliptical nor dynamical states appear. It is clearly evident from Fig. 7 that the current interval in which dynamical states appear (the region delimited by the crosses and triangles) decreases for increasing detuning. The latter observation is in qualitative agreement with the experiments performed for increasing device temperature, which is known to result in an increase of the detuning as it is defined by Eq. (4). The appearance of the dynamical states has been checked to be robust against variations of β_{sp} ($10^{-4} \leqslant \beta_{sp} \leqslant 10^{-12}$ ns^{-1}). However, the point of the PS is slightly changed by a variation of this quantity.

For $\Delta < 0$, Fig. 7 shows that there is a region in parameter space, in which no linearly polarized SOP is stable. As in the scenario considered before, first an elliptically polarized steady state is emitted, if the LF-mode becomes unstable. This state then is replaced by a dynamical state. For these parameters, the HF-mode with linear SOP becomes stable at high currents. However, the stabilization of the HF mode does occur only at very high current levels, since the stability boundary of the HF-mode is nearly vertical at the low detuning side. Fig. 8(b) shows a LI-curve in the $\Delta < 0$ region. In contrast to the case $0 \leqslant \Delta < 1$, there is a switch-over between dominance of the polarization direction corresponding to the LF-mode and dominance of the orthogonal linear polarization direction (here at $\mu \approx 8.6$) within the region with dynamical states. This switch-over takes place rather abruptly for a current value less than the

one at which the HF-mode becomes stable. For $\mu > 12.3$, the linearly polarized HF-mode is operating.

In experiments, the point of PS is often defined as the current level at which equal power is observed for projection onto two orthogonal linear SOP. By using the above definition, the scenario observed for $\Delta < 0$ can be considered as a possible explanation for the observation of dynamical states after a PS (Fig. 5, see also [15,21]).

The discussion of the theoretical results so far has been restricted to situations where the LF-mode is lasing at threshold. However, the experiments have demonstrated that dynamical states can exist also if the lasing LF-state is already the result of a PS after the HF-mode had emerged at threshold (double switching scenario). In the following we will discuss the possibility to observe the latter scenario in the model used here. One possibility is to allow for a drift of the detuning proportional to the injection current, as it is the case for cw-operation in the experiments. With an appropriate choice of the parameters, the system follows a path like the one indicated by the arrow labelled (a) in Fig. 9: At threshold, the HF-mode is lasing, as predicted by the LSA. If the current is increased, a PS to the LF-mode occurs. This mode is lasing, until the regime of instability is reached and the VCSEL transits to the elliptically polarized steady state which is replaced by the dynamical state. Finally, the laser switches to the HF-mode after exiting the instability region.

A second possibility to observe dynamical states at the 2nd PS of a double-PS scenario is for the case of fixed detuning and the VCSEL passing through a bistability region (depicted by the arrow labelled (b) in Fig. 9). In a purely deterministic system, no PS is expected along this path since the HF-mode is always (linearly) stable. Nevertheless, we find numerically the possibility of a PS, if noise terms are included. The reason is that – though both the HF- and the LF-state are linearly stable – the damping of perturbations that are orthogonally polarized to the HF-state is much weaker than the damping of the perturbations that are orthogonally polarized to the LF-state [26]. Hence, the LF-state is preferred, if the spontaneous emission noise is strong enough to force the system

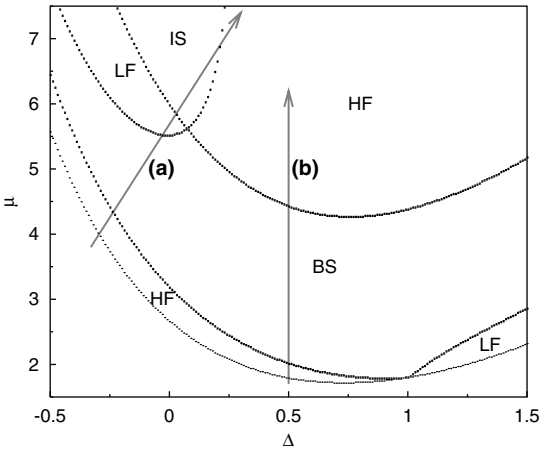

Fig. 9. Same as Fig. 7, but for different parameters: $\gamma_a = -0.5$ ns^{-1}, $\gamma_p = 20$ ns^{-1}, $\gamma_j = 22$ ns^{-1}, $A = 0.5$ ns^{-1}, $B = 1$ ns^{-1}, $\kappa = 300$ ns^{-1}, $a = 2.5 \times 10^4$ ns^{-1}, $\gamma_\perp = 10^4$ ns^{-1}.

to this mode within the bistability region. This mode will remain lasing until the upper boundary of the bistability region, where it becomes unstable. From here on the scenario is the same as for the case where the LF-mode is lasing at threshold. However, this second scenario is very sensitive to the magnitude of β_{sp}. For example, for the parameters of Fig. 9 the double PS is observed for $\beta_{sp} = 3 \times 10^{-6}$ ns^{-1} and larger values. Already for a decrease of β_{sp} to 2×10^{-6} ns^{-1} the double PS is not observed any more, i.e., the HF-mode is always lasing.

Finally, we want to highlight the influence of the spin-flip rate γ_j on the dynamics. An increase (decrease) of γ_j results in an increase (decrease) of the current value for which the LF-mode becomes unstable. Consequently, the current values at which the elliptically polarized steady state and the dynamical states occur increase (decrease). A similar conclusion was obtained in a recent paper [29] treating PS in optically pumped long-wavelength VCSELs. These authors relate the fact that they do not observe elliptically polarized states to the fact that the spin-flip rate in InGaAs/InP quantum wells is known to be larger than in GaAs/AlGaAs quantum wells (the type which 850 nm-lasers are based on, see [29] and references therein).

4. Discussion

The experimental results indicate that the occurrence of the dynamical states is not necessarily connected to a certain amount of ellipticity of the SOP at threshold (indeed, the dynamical states have also been shown to occur, if the SOP at threshold is linear, see Fig. 2). Therefore, a comparison to the model treated in the preceding section, which accounts only for a linear SOP at the lasing threshold, seems to be justified. The appearance of elliptically polarized and dynamical transition states in the vicinity of a PS from the LF- to the HF-mode is very different from the PS scenario from the HF- to the LF-mode, where these states are neither reported experimentally nor expected from the SFM-model.

In our opinion, the asymmetry between the two switching scenarios is due to the different mechanism of destabilization of the lasing mode. The linearly polarized steady state is characterized by equality of D_+ and D_- [12,30], which is valid for both the LF- and the HF-mode. Elliptically polarized steady states are characterized by $D_+ \neq D_-$ [12]. For linearly polarized states, the stability of the total intensity decouples from the stability of the polarization subset. The stability of the linearly polarized modes against perturbations with orthogonal polarization and/or a deviation from $D_+ = D_-$ is expressed by the three remaining eigenvalues. Two of these are complex conjugate, the third eigenvalue is real. The real eigenvalue is (at least in the case of relatively large spin relaxation rates) mainly associated with perturbations of the equality of D_+ and D_- [22,24]. In the case of switching from the HF- to the LF-mode and for the parameter combinations we have studied (e.g. the parameters used here and also the ones used in [25,26]), it is always the complex conjugate eigenvalue that acquires a positive real part and hence leads to destabilization of the HF-mode (see also [12]). The real eigenvalue is always negative, what implies stability of the condition $D_+ = D_-$. Hence, elliptically polarized states cannot be expected. For the PS from the LF- to the HF-mode, the behaviour of the eigenvalues is different. There exist two possibilities how the linearly polarized LF-mode can lose linear stability. One possibility is that the real eigenvalue becomes positive, i.e., perturbations with $D_+ \neq D_-$ are not damped. This is the case for the parameters of Figs. 6, 7 and 9. The other possibility is that the imaginary part of the complex conjugate eigenvalues becomes zero at increasing current. For the case of adiabatic elimination of the spin dynamics this has been shown analytically in [24]. The linearly polarized LF-mode becomes unstable when one of the three – now real – eigenvalues becomes positive. Also in this case, the positive eigenvalue is the eigenvalue that is already real at threshold. It has also been shown in [12] (for the case of no linear dichroism) that the LF-mode is destabilized by a real eigenvalue. To our best knowledge, there are no parameter combinations that allow other scenarios than the ones described here. For completeness, it should be noted that the three eigenvalues discussed above do not determine the domain of linear stability of the elliptical (steady) states. In the latter case, intensity and polarization dynamics do not decouple and one has to consider five eigenvalues [12].

The qualitative similarities between the temporal dynamics observed in the experiments and the simulations suggest that the oscillations observed for projection onto a linear SOP are caused by (irregular) oscillations of the polarization angles at constant current. These fluctuations are the natural cause for the decrease of the fractional polarization that is observed for the dynamical states in the simulations. Furthermore, it has been shown that the model used for comparison here is able to qualitatively reproduce the two-dimensional (current and detuning or temperature, respectively) existence region that was observed in experiments. We mention that the transient dynamics of a PS from the LF- to the HF-mode was investigated and oscillations of the Stokes parameters were found in [31], which are in agreement with predictions of the SFM-model. However, in this paper the authors do not comment on the scenario before the PS.

The results of the linear stability analysis (Figs. 7 and 9) show the existence of a region were none of the two orthogonal linearly polarized modes is stable. There exists the possibility that this region does not close for increasing current (see Fig. 9),

i.e., the laser does not return to a linearly polarized steady state. This scenario is probably related to the experimental observation reported in Fig. 4. However, in the experiment we can only demonstrate that the operation with dynamical states does not cease before we enter the current region in which high-order transverse modes are excited. At this point, a comparison between experiment and theory is no longer meaningful.

Also the experimentally observed double-PS, including the dynamical states at the second PS, can be explained within the framework of this model. The question which one of the two scenarios (arrows (a) and (b) in Fig. 9) is actually observed in the experiment is difficult to answer. Indeed, under the experimental condition of cw-operation the detuning is continuously increasing, if the current is increased. But this fact does not a priori exclude the scenario (b) of Fig. 9, since the latter is also possible if a detuning drift with current is included, i.e., with a tilt of arrow (b) the double PS can still be observed, if the noise is strong enough to induce the first PS.

We note that double-PS can also be observed within the original SFM. However, it has been shown to be necessary to include gain saturation if the second PS (the type II PS) should occur at reasonably low current values in the absence of noise [32].

5. Conclusions

To conclude, we have given an experimental characterization of elliptically polarized dynamical states in the polarization dynamics of VCSELs. These states manifest themselves in sidebands in the optical spectrum, peaks in the rf-spectrum at integer multiples of the sideband distance, temporal fluctuations at these frequencies for projection onto linear polarization and a pronounced decrease of the fractional polarization. The experimental observations have been reproduced qualitatively and explained within the framework of a model that includes spin-flip dynamics as well as the frequency dependence of the dielectric susceptibility of the semiconductor gain material and the complex nature of the electromagnetic field.

There remains the important question whether the experimental observations can be explained by other models that do not incorporate spin-flip processes. However, to our best knowledge there are no reports of other models that predict the appearance of elliptical and dynamical states at a PS. In particular, in a model that is based on rate equations for the mode *intensities* a transition between linear and elliptical polarization cannot occur. Since we can treat and explain several aspects of the behaviour of the elliptically polarized states in the model used here, we conclude that it is important to account for phase degrees of freedom *and* a non-linear mechanism. The SFM supplies these two important ingredients. The observed qualitative similarities of the experimental results and the (extended) SFM are a strong indication that spin dynamics decide about the state of polarization in the devices we have investigated.

Acknowledgements

The experimental work was supported by the Deutsche Forschungsgemeinschaft and the collaboration between the groups was possible due to travel grants by the Deutsche Akademische Austauschdienst, the COST Action 268 and the Deutsche Forschungsgemeinschaft. The raw data for Figs. 1 and 4 were obtained by M.S. during a visit at the Vrije Universiteit Brussels. He is grateful to J. Danckaert and G. Verschaffelt for the hospitality.

References

[1] M. San Miguel, in: A. Miller, M. Ebrahimzadeh, D.M. Finlayson (Eds.), Semiconductor Quantum Optoelectronics: From Quantum Physics to Smart Devices, SUSSP and Institute of Physics Publishing, Bristol, 1999, p. 339.
[2] A.K.v. Doorn, M.P.v. Exter, J.P. Woerdman, Appl. Phys. Lett. 69 (1996) 1041.
[3] R.F.M. Hendriks, M.P.v. Exter, J.P. Woerdman, A.v. Geelen, L. Weegels, K.H. Gulden, M. Moser, Appl. Phys. Lett. 71 (1997) 2599.
[4] C.J. Chang-Hasnain, J.P. Harbison, G. Hasnain, A. von Lehmen, L.T. Florez, N.G. Stoffel, Electron. Lett. 27 (1991) 163.
[5] K.D. Choquette, D.A. Richie, R.E. Leibenguth, Appl. Phys. Lett. 64 (1994) 2062.

[6] M.P.v. Exter, M.B. Willemsen, J.P. Woerdman, Phys. Rev. A 58 (1998) 4191.
[7] M.B. Willemsen, M.U.F. Khalid, M.P.v. Exter, J.P. Woerdman, Phys. Rev. Lett. 82 (1999) 4815.
[8] K. Panajotov, B. Nagler, G. Verschaffelt, A. Georgievski, H. Thienpont, J. Danckaert, I. Veretennicoff, Appl. Phys. Lett. 77 (11) (2000) 1590.
[9] K. Panajotov, B. Ryvkin, J. Danckaert, M. Peeters, H. Thienpont, I. Veretennicoff, IEEE Photon. Technol. Lett. 10 (1998) 6.
[10] B. Ryvkin, K. Panajotov, A. Georgievski, J. Danckaert, M. Peeters, G. Verschaffelt, H. Thienpont, I. Veretennicoff, J. Opt. Soc. Am. B 16 (1999) 2106.
[11] M.S. Miguel, Q. Feng, J.V. Moloney, Phys. Rev. A 52 (1995) 1728.
[12] J. Martín-Regalado, F. Prati, M.S. Miguel, N.B. Abraham, IEEE J. Quantum Electron. 33 (1997) 765.
[13] T. Erneux, J. Danckaert, K. Panajotov, I. Veretennicoff, Phys. Rev. A 59 (1999) 4660.
[14] F. Prati, M. Bache, F. Castelli, Europhysics Conference Abstracts 27E (2003) EA4T;
F. Prati, P. Caccia, M. Bache, F. Castelli, Analysis of elliptically polarized states in vertical-cavity-surface-emitting lasers, PRA, in press.
[15] T. Ackemann, M. Sondermann, Appl. Phys. Lett. 78 (2001) 3574.
[16] S. Balle, Phys. Rev. A 57 (1998) 1304.
[17] S. Balle, E. Tolkacheva, M.S. Miguel, J.R. Tredicce, J. Martín-Regalado, A. Gahl, Opt. Lett. 24 (1999) 1121.
[18] M. Travagnin, Phys. Rev. A 56 (1997) 4094.
[19] A.K.v. Doorn, M.P.v. Exter, A.M.v.d. Lee, J.P. Woerdman, Phys. Rev. A 55 (1997) 1473.
[20] K. Panajotov, H. Thienpont, I. Veretennicoff, Enhanced polarization control and stabilization by microscopic in-plane anisotropic strain in vertical-cavity surface-emitting lasers, US patent US2003/0075725 A1, 2003.
[21] T. Ackemann, M. Sondermann, Proc. SPIE 4286 (2001) 44.
[22] H. Lem, D. Lenstra, Opt. Lett. 22 (1997) 1698.
[23] H.F. Hofmann, O. Hess, Quantum Semiclass. Opt. 10 (1998) 87.
[24] M.P.v. Exter, R.F.M. Hendricks, J.P. Woerdman, Phys. Rev. A 57 (1998) 2080.
[25] M. Sondermann, M. Weinkath, T. Ackemann, J. Mulet, S. Balle, Phys. Rev. A 68 (2003) 033822.
[26] M. Sondermann, M. Weinkath, T. Ackemann, IEEE J. Quantum Electron. 40 (2004) 97.
[27] J. Mulet, S. Balle, IEEE J. Quantum Electron. 38 (3) (2002) 291.
[28] J. Mulet, S. Balle, Phys. Rev. A 66 (2002) 053802.
[29] Y. Matsui, D. Vakhshoori, P. Wang, P. Chen, C.-C. Lu, M. Jiang, K. Knopp, S. Burroughs, P. Tayebati, IEEE J. Quantum Electron. 39 (2003) 1037.
[30] M. San Miguel, S. Balle, J. Mulet, C. Mirasso, E. Tolkachova, J.R. Tredicce, Proc. SPIE 3944 (2000) 242.
[31] M.B. Willemsen, M.P.v. Exter, J.P. Woerdman, Phys. Rev. Lett. 84 (2000) 4337.
[32] F. Prati, P. Caccia, F. Castelli, Phys. Rev. A 66 (2002) 063811.